ELSEVIER

Journal of Magnetism and Magnetic Materials 161 (1996) 49–56

journal of magnetism and magnetic materials

Interface roughness in Fe(100)/Cr film structures studied by CEMS

F. Klinkhammer, Ch. Sauer *, E.Yu. Tsymbal, S. Handschuh, Q. Leng, W. Zinn [1]

Institut für Festkörperforschung, Forschungszentrum Jülich GmbH, D-52425 Jülich, Germany

Received 3 October 1995; revised 28 November 1995

Abstract

Various epitaxial Fe(100)/Cr film structures were MBE-grown on MgO(100) and GaAs(100) substrates with the aim to modify the roughness of the Fe/Cr interfaces. By introducing a 2 monolayer thick ^{57}Fe probe layer at the interface the distribution of the magnetic hyperfine (hf) fields could be measured locally by means of ^{57}Fe conversion electron Mössbauer spectroscopy (CEMS). A simple model is applied which allows the determination of a pattern of the average interface roughness from this hf field distribution. It was observed that even samples of high epitaxial quality according to LEED and RHEED reveal a micro-roughness on a lateral scale of 1–2 nm due to intermixing of Fe and Cr within 1–2 monolayers.

PACS: 68.55.Bd; 68.65.+g; 75.70.Cn; 76.80.+y

Keywords: Mössbauer effect; CEMS; Interface roughness; Fe(100)/Cr; Layered structures

1. Introduction

Metallic magnetic multilayers with antiferromagnetic (AFM) interlayer coupling [1] have attracted considerable interest in recent years. This is mainly due to the 'giant' magnetoresistance effect (GMR) which can occur in such systems and was detected first in Fe/Cr/Fe film structures [2,3]. It is known that the GMR [4] as well as the magnetic interlayer coupling is strongly influenced by the structure of the interfaces separating the magnetic and non-magnetic layers within the film system. For example, while interface roughness can cancel the short wave oscillations of the 180° AFM coupling, most of the proposed models for the 90° coupling are based on the existence of roughness [5,6] or moderate interdiffusion [7] at the interfaces. On this background it would be interesting to analyze the roughness and interdiffusion at interfaces in magnetic film structures. A first information on the structural quality of the interfaces can be gained by RHEED and LEED during the sample preparation. X-ray scattering under grazing incidence [8] is a useful method which yields the average height and lateral extension of steps (= roughness) at interfaces. It has been applied recently to epitaxial Fe(100)/Cr multilayers by Schreyer et al. [9] to gain informations on the length scale of constant Cr layer thickness. But in this case,

* Corresponding author. Fax.: +49-2461-61-2016; email: ch.sauer@kfa-juelich.de.

[1] Deceased 13 April 1995.

PII S0304-8853(96)00063-7

due to the weak contrast between Fe and Cr, multilayers including more than one interface are necessary. For such investigations microscopic nuclear methods like γ–γ perturbed angular correlation (PAC), nuclear magnetic resonance (NMR) or conversion electron Mössbauer spectroscopy (CEMS) are powerful tools. By introducing suitable tracer atoms at the interface the roughness and interdiffusion can be analyzed locally quite in detail.

In this work we have prepared epitaxial Fe(100)/Cr film structures under various preparation conditions and performed ^{57}Fe CEMS investigations. In order to modify the interface roughness, samples were grown on two different substrates (GaAs(100) and MgO(100)) and at different substrate temperatures. The Fe films were made from the non-Mössbauer isotope ^{56}Fe. Directly at the Fe/Cr interface a 2 monolayer (ML) thick ^{57}Fe layer was inserted for probing the local structure. ^{57}Fe atoms sitting, e.g., at the edges of steps will see a different hyperfine (hf) field compared to probe atoms sitting within flat regions at the interface. Therefore, the hf field can serve as a fingerprint of the various Fe–Cr neighbor configurations. The resulting CEMS spectra consist of a superposition of different subspectra reflecting these individual Fe–Cr configurations. We propose a model for the interpretation of such CEMS spectra which allows the visualization of an average roughness pattern of the investigated interface.

2. Experimental

Several groups [10–13] have reported on the successful growth of Fe/Cr multilayers on MgO(100) substrates. We have prepared thin film structures of Fe(100)/Cr by evaporation in ultra high vacuum (UHV) on MgO(100) and GaAs(100) substrates with buffer layers of 40 nm Cr (MgO) and 150 nm Ag (GaAs), respectively. The preparation of the GaAs based systems as sketched in Fig. 2 is described elsewhere [14]. Fig. 1 shows the structure of the MgO based films. The MgO(100) single crystalline platelets with dimensions of $10 \times 10 \times 0.5$ mm were heated for 24 h at 1050°C in air in order to reconstruct surface deteriorations arising by storage in air. After this treatment atomic force microscopy revealed a vertical surface roughness of 0.2–0.4 nm and a terrace width of ~ 200 nm. Immediately after the heating the substrate was introduced into the

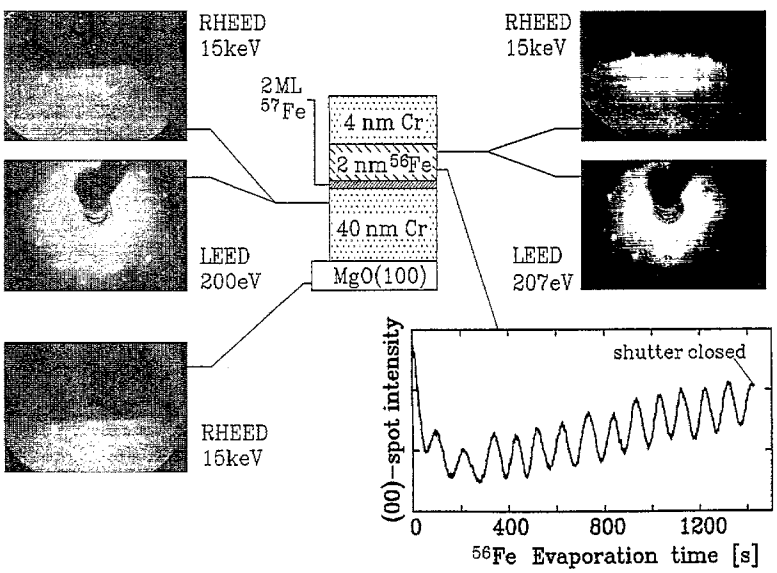

Fig. 1. Structure of the MgO based thin film samples with RHEED pattern of the MgO substrate after heat treatment, LEED and RHEED patterns of the Cr buffer layer and the ^{56}Fe film, respectively. The RHEED oscillations registered during the growth of the ^{56}Fe film are shown also.

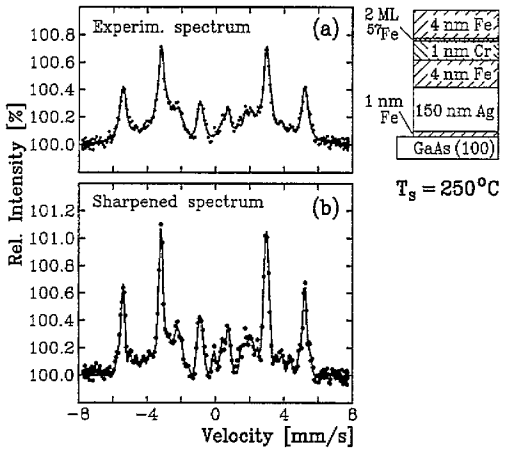

Fig. 2. Structure of the GaAs based sample grown at $T_s = 250°C$ and the related experimental CEMS spectra as measured (a) and after line sharpening (b). See text.

UHV preparation chamber with a base pressure around 1×10^{-8} Pa. Carbon contamination of the surface usually emerging from the MgO bulk during the heating was detected by Auger spectroscopy and removed by sputtering with 700–1000 eV Ar ions. Such carbon contamination leads to various reconstructions of the afterwards evaporated films depending on the C-concentration [15]. Then, the cleaned substrate was heated to 700°C for annealing the surface. The RHEED pattern of the substrate after this treatment shows very sharp spots located on a Laue circle indicating an excellent flat surface (Fig. 1). In order to reduce the lattice mismatch of 3.7% between MgO and Fe and to improve the epitaxial growth of the Fe/Cr structure a 40 nm thick Cr buffer layer was grown on the MgO at 700°C increasing the evaporation rate from 2×10^{-3} nm/s for the first 2 nm Cr thickness to 3×10^{-2} nm/s. The bcc-Cr grows on MgO (NaCl structure) with a rotation of the (100) plane by 45°. The LEED and RHEED patterns of this Cr buffer layer (Fig. 1) are not as good as of the MgO platelet but reveal still a very flat surface with a $p(1 \times 1)$ structure. The high substrate temperature of 700°C gave the best quality of the Cr-buffer. The following ^{57}Fe probe layer and the ^{56}Fe layer were grown usually at 190–200°C with an evaporation rate of 2×10^{-3} nm/s. At this temperature nearly no interdiffusion of Fe/Cr and ^{56}Fe/^{57}Fe was found [16]. Though the LEED and RHEED patterns become slightly worse (Fig. 1) the observed RHEED oscillations indicated layer by layer growth of the Fe-films. On the other hand, during the growth of the Cr buffer RHEED oscillations could be observed at 250°C substrate temperature only, but not at the optimum temperature of 700°C due to the high inelastic background. The 4 nm thick Cr layer on top of the film structure served as corrosion protection.

Using a 50 nm thick Ag buffer layer on MgO instead of the Cr buffer an equally good epitaxial growth of the Fe/Cr structure could be achieved. The Ag buffer was grown at 150°C with 2×10^{-3} nm/s evaporation rate and annealed at 330°C for 1 hour before growing the Fe/Cr structure. Between MgO substrate and Ag buffer an 1 nm thick seed layer of Fe or Cr was needed for improving of the Ag sticking. However, there was a problem with Ag buffers due to the slight segregation of Ag atoms through the following Fe- or Cr-layer leading to an Ag surface contamination.

Small Al_2O_3 crucibles were used for the evaporation of the Fe-isotopes and an electron beam heated W-crucible for the Cr evaporation. The film thickness could be controlled with an accuracy of $\sim 5\%$ using individual quartz oscillators for each crucible. By moving an additional quartz at the substrate position the quartz calibration could be checked quickly. In order to vary the interface roughness, substrate temperatures of 90°C and 190°C were applied for the growth of the Fe/Cr structure for the MgO system and of 20°C and 250°C for the GaAs system, respectively. Also, the ^{57}Fe probe layer was inserted alternatively at the lower or at the upper Fe/Cr interface. The CEMS measurements were performed at $T = 300$ K in UHV using 40 mCi (^{57}Co)Rh as γ-source and a channeltron for the detection of the conversion electrons.

3. Results and discussion

As an example, Fig. 2a shows the experimental CEMS spectrum of an Fe/Cr interface grown at 250°C on GaAs(100). The spectrum was fitted (solid line) by a superposition of 10 magnetically split subspectra with isomer shift, hf field, quadrupole

interaction, Lorentzian line width (assumed to be equal for all 6 lines within one subspectrum) and relative intensity (area) of the subspectra as free fitting parameters. Alternatively, the experimental spectrum was sharpened first by applying the integral transformation procedure suggested by Afanas'ev and Tsymbal [17] for an improvement of the spectral resolution. Then, the sharpened spectrum was fitted in the same manner, however, assuming Gaussian line shape (solid line in Fig. 2b). Both methods gave the same results within the limits of error, but the data derived by the sharpening procedure were more stable. The CEMS spectra of totally about 20 Fe/Cr film samples were treated in this way. As a result, it was found that all these interface spectra could be fitted quite well assuming a common set of 10 values of the hf field and isomer shift. This finding suggests that all Fe/Cr interfaces have some identical structural features and differ only in the relative intensity of the individual subspectra contributing to the total CEMS spectrum.

It is known that Fe–Cr alloys mix nearly homogeneously within the whole concentration range. The hf field B_{hf} of the Fe atoms in these alloys decreases with increasing Cr concentration and can be described empirically [18] by the simple relationship $B_{hf} = B_{bulk} + n_1 B_1 + n_2 B_2$. Here, $B_{bulk} = -33.3$ T (at $T = 300$ K) denote the hf field of bulk-Fe and $B_1 = 3.19$ T and $B_2 = 2.15$ T the hf field contributions of the n_1 Cr atoms in the nearest (n.n.) and n_2 Cr atoms in the next nearest neighbor (n.n.n.) shell around the Fe ad-atom, respectively. The negative sign refers to the direction of the magnetization. Third nearest Cr neighbors are neglected. In principle, one could expect that an Fe/Cr interface revealing some roughness behaves similar to an Fe–Cr alloy. On this idea first attempts were based to fit the CEMS spectra of Fe(110)/Cr interfaces [19], however, with moderate success, because those spectra could be resolved in 4 subspectra only.

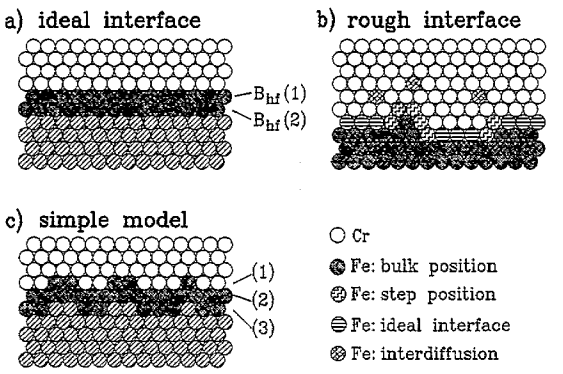

Fig. 3. Schematic models of Fe/Cr interfaces marked by 2 ML ^{57}Fe: (a) ideal flat interface revealing two hf. field values only; (b) rough interface comprising ideal, step and bulk positions as well as interdiffusion of the ^{57}Fe atoms; (c) simple model as used for the interpretation of the CEMS spectra.

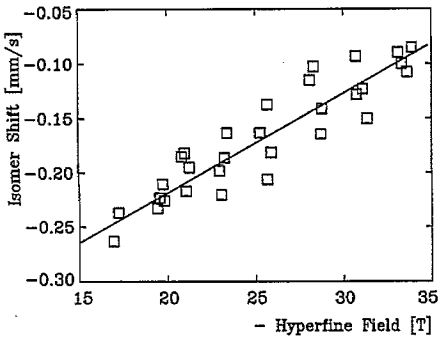

Fig. 4. Isomer shift of the subspectra (referred to a ^{57}Co/Rh γ-source) as a function of the corresponding hf. field. The data of 4 different samples are compiled.

Now, the improved resolution and the deconvolution of the experimental spectrum in 10 discrete subspectra offers the opportunity to refine the alloy model. For an ideally flat interface marked with a 2 ML thick ^{57}Fe probe layer (see Fig. 3a) one would expect a CEMS spectrum consisting of two subspectra with hf field values attributed to the direct Fe interface layer $B_{hf}(1)$ and to the second ^{57}Fe layer $B_{hf}(2)$. At a rough interface, however, there exists a variety of ^{57}Fe positions, e.g., at the corners or edges of steps or at flat regions (Fig. 3b). According to their individual Fe–Cr neighbor configurations these different positions will exhibit different hf field values. In a crystalline bcc-lattice one can count 10 different positions and related Fe–Cr configurations when the roughness is restricted to one-atomic steps only. Of coarse, interdiffusion can occur also. Therefore, the hf fields can serve as a fingerprint of the local Fe–Cr neighbor configurations. This interpretation is supported by a plot of the isomer shift of the subspectra as a function of the affiliated hf field (Fig. 4) revealing a linear dependence. Due to the larger electronegativity of Fe compared with Cr, the s-elec-

tron density at the Fe-nuclei is expected to increase with increasing number of Cr neighbors giving a more negative isomer shift. Simultaneously, the hf field decreases with increasing number of Cr neighbors.

As mentioned before, the CEMS spectra of our Fe/Cr specimens could be fitted using a common set of hf fields. In analogy to the alloy model we could describe this set of hf fields by the modified relationship

$$B_{\mathrm{hf}} = B_{\mathrm{bulk}} + n_1 B_1 + n_2 B_2 + \Delta B + \Delta B_{(i=2)}. \qquad (1)$$

Again, $B_{\mathrm{bulk}} = -33.3$ T (at $T = 300$ K) and n_1 and n_2 are defined as before. However, the neighbor contributions change to $B_1 = 2.5$ T and $B_2 = 2.05$ T. In addition a constant contribution $\Delta B = -1.75$ T must be introduced, which probably reflects the usually observed enhancement of the hf field at Fe/metal interfaces [20] due to the broken translational symmetry. Solely for the second ^{57}Fe ML at the interface ($n_1 = 0$, $n_2 = 1$) a further contribution $\Delta B_{(i=2)} = -1.2$ T is required which is zero for all the other positions. Eq. (1) holds for ^{57}Fe positions at the interface only, but not for the Fe-bulk positions. The necessary modifications as introduced in Eq. (1) demonstrate that, obviously, a homogeneous alloy can be compared with a rough interface in a rough approximation only. It should be emphasized that this evaluation procedure is empirical and is justified only by the success in describing the experimentally observed hf fields fairly well. The hf fields as calculated by Eq. (1) for the ^{57}Fe positions differing by the number of nearest (n_1) and next nearest (n_2) Cr neighbors are compiled in Table 1.

Beside the calculation of the hf fields for the individual Fe–Cr configurations also the probability of occurrence of the configurations is needed in order to obtain a roughness pattern of the interface.

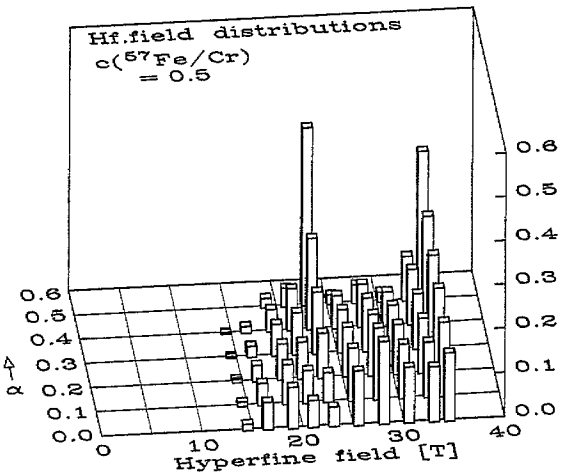

Fig. 5. Hyperfine field distributions as calculated using the model described in the text for a ^{57}Fe concentration $c = 0.5$ and various α-values.

According to Fig. 3c we used a model where the 2 ML thick ^{57}Fe probe layer is distributed across 3 monolayers. One monolayer (no. 2) in the center is completed with ^{57}Fe atoms, the monolayer (no. 1) adjacent to the Cr film has the concentration c of ^{57}Fe atoms and the third monolayer (no. 3) adjacent to the ^{56}Fe film the ^{57}Fe concentration (1-c), respectively. While layer no. 3 consists of Fe atoms (^{56}Fe and ^{57}Fe) only, the layer no. 1 has an alloy character containing ^{57}Fe and Cr atoms, and reflects the roughness pattern within this simple model. The detailed distribution of ^{57}Fe atoms in the alloy-like monolayer no. 1 is determined using a short range order parameter α. This parameter refers to n.n.n. pairs only, because in the same (100) plane (no. 1) no nearest neighbor sites exist. All n.n. atoms are located in the adjacent (100) planes, i.e., they are either Fe or Cr atoms according to the model. The

Table 1
Hf field values as calculated by Eq. (1) for different ^{57}Fe positions at the Fe(100)/Cr interface assuming one-atomic steps only. n_1 and n_2 denote the numbers of n.n. and n.n.n. Cr-neighbor atoms

	Interface positions of ^{57}Fe				^{57}Fe in 2nd or 3rd layer					
n_1	4	4	4	4	4	3	2	1	0	0
n_2	5	4	3	2	1	1	1	1	1	0
$-B_{\mathrm{hf}}$ (T)	14.8	16.9	18.9	21.0	23.0	25.5	28.0	30.5	34.2	33.3

probability p of finding an ^{57}Fe atom at a particular n.n.n. site within the ^{57}Fe–Cr alloy layer is given by

$$p = c + \alpha(1 - c). \quad (2)$$

The parameter α can range from 0 to 1. It describes the degree of clustering (ordering) of the ^{57}Fe atoms within the interface monolayer. Complete randomness relates to $\alpha = 0$, and $\alpha = 1$ corresponds to total Fe–Cr separation.

Within this model a distinct roughness pattern, i.e., a distinct distribution of ^{57}Fe and Cr atoms in the interface layer is characterized by the two parameters c and α. By using Eq. (1) and Eq. (2) the hf field distribution belonging to that specific roughness pattern can be calculated. Fig. 5 shows as an example the calculated hf field distributions for $c = 0.5$ and different α-values. Then, by comparison of the experimental hf field distribution as derived from the CEMS spectrum with the calculated B_{hf} distributions one obtains the c and α parameters and the roughness pattern. This procedure is demonstrated in Fig. 6. Here, the experimental hf field distribution evaluated from the CEMS spectrum displayed in Fig. 2 is plotted together with the best fitting model distribution. From the parameters $c = 0.5$ and $\alpha = 0.3$ derived in this way a roughness pattern of the interface can be constructed as shown in Fig. 7a. This pattern is a top view on the alloy-like interface monolayer. It represents a visualization of the interface roughness giving a picture of the average Fe–Cr distribution and clustering, but not a real scan or image of the interface.

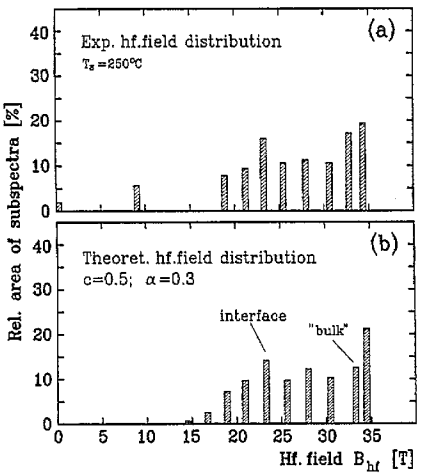

Fig. 6. (a) Experimental hf field distribution as determined from the sharpened CEMS spectrum shown in Fig. 2b. (b) Calculated hf field distribution which fits best to the experimental distribution yielding $c = 0.5$ and $\alpha = 0.3$.

Table 2 compiles the results of the interface roughness analysis for several thin Fe(100)/Cr film systems prepared under various conditions. The GaAs based sample no. 2 prepared at $T_s = 250$°C revealed a slightly reduced roughness, but increased interdiffusion compared with sample no. 1 prepared at 20°C. Usually it was observed that the GaAs/Ag-buffer samples prepared at 250°C show an enhanced 90°

Table 2
Results of the parameters c and α characterizing the interface roughness, and of the ^{57}Fe interdiffusion ID for different Fe(100)/Cr samples. T_s = substrate temperature during the growth of the Fe/Cr structure

No.	Substrate	T_s	Position of ^{57}Fe probe layer	c	α	ID [a]	Remark
1	GaAs	20°C	Ag-buffer/^{56}Fe/Cr/^{57}Fe/^{56}Fe	0.6	0.2	5%	
2	GaAs	250°C	Ag-buffer/^{56}Fe/^{57}Fe/Cr/^{56}Fe	0.5	0.3	9%	
3	MgO	90°C	Cr-buffer/^{57}Fe/^{56}Fe/Cr	0.5	0.1	8%	b
4	MgO	190°C	Cr-buffer/^{57}Fe/^{56}Fe/Cr	0.6	0.1	10%	c
5	MgO	190°C	Cr-buffer/^{57}Fe/^{56}Fe/Cr	0.6	0.1	9%	d
6	MgO	190°C	Cr-buffer/^{56}Fe/^{57}Fe/Cr	0.6	0.2	5%	e
7	MgO	190°C	Ag-buffer/^{56}Fe/^{57}Fe/Cr	0.6	0.2	5%	f

[a] ID = Fe–Cr interdiffusion (relative contribution of paramagnetic subspectrum).
[b] ^{57}Fe probe layer grown directly on the Cr-buffer.
[c] Stop of growth of the Cr-buffer at the maximum of the RHEED oscillation and then start of ^{57}Fe growth.
[d] Stop of growth of the Cr-buffer at the minimum of the RHEED oscillation and then start of ^{57}Fe growth.
[e] ^{57}Fe probe layer at the upper Fe/Cr interface (see Fig. 1).
[f] ^{57}Fe probe layer at the upper Fe/Cr interface (see Fig. 1) and Ag-buffer on MgO (instead of Cr-buffer).

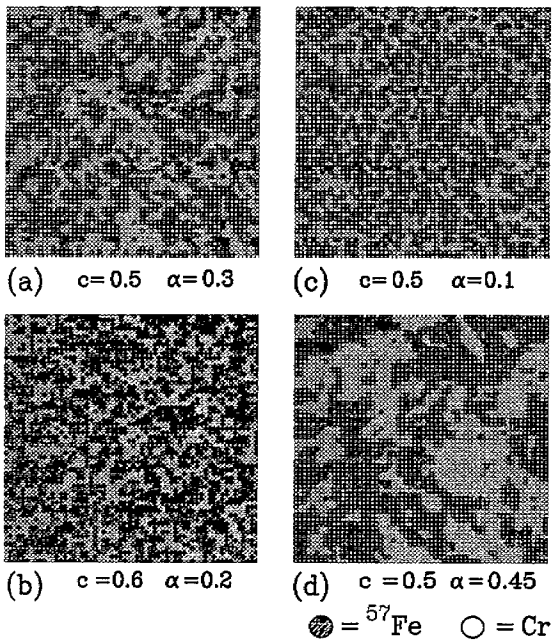

Fig. 7. Patterns of the interface roughness simulated using the parameters c and α as derived from the hf field distributions. The patterns correspond to (a) sample no. 2 in Table 2; (b) sample no. 1; and (c) sample no. 3. For comparison, a roughness pattern for $c = 0.5$ and $\alpha = 0.45$ is shown in Fig. 7d.

interlayer coupling [14]. Thus, our observation of a slightly increased diffusion of Fe atoms into the Cr interlayer supports the 'loose spin' model of Slonczewski [7] explaining the 90° coupling by paramagnetic spins in the nonmagnetic interlayer. The MgO based samples no. 4 and 5 were prepared as follows. After completing the Cr-buffer layer grown at 700°C a few additional Cr layers were added at $T_s = 200$°C in order to make visible RHEED oscillations. Then the Cr-growth was stopped at the maximum (sample no. 4) and the minimum intensity (no. 5) of the RHEED oscillation, respectively. The maximum of the RHEED intensity indicates maximum reflection of the electron beam and, therefore, the completion of a monolayer, while minimum intensity characterizes a half-filled and rough surface layer. According to Table 2 there was virtually no difference in interface roughness observed between these two specimens. A slightly less roughness was found when the ^{57}Fe probe layer was inserted at the upper Fe/Cr interface (samples no. 6 and 7). This may be due to the fact, that the first three Fe monolayers grow on Cr in a 3-dimensional mode, while ^{57}Fe on ^{56}Fe continues the layer by layer growth mode.

Generally, all investigated samples showed a pronounced micro-roughness of the Fe/Cr interface with continuous Fe or Cr regions not larger than ~ 10 atoms. The largest value found for the short range order parameter was $\alpha = 0.3$. Obviously, there exists an intermixing between Fe and Cr within 1–2 monolayers at the interface. Such an intermixing could occur during the evaporation by a site exchange of the Cr atoms and the incoming Fe atoms. This finding seems to be in contrast to the RHEED and LEED patterns obtained during the film preparation, which indicated good epitaxial quality with an average width of terraces of 5–10 nm. But due to the weak difference of the electron scattering probability between Fe and Cr, LEED and RHEED should be not sensitive for resolving the chemical roughness. Detailed STM (scanning tunneling microscopy) investigations of the growth of Fe [21] and Cr [22] on Fe(100) whiskers agree generally with our roughness patterns. Furthermore, using ^{57}Fe-CEMS Schurer et al. [23] observed also a similar chemical micro-roughness at the interfaces in Fe(100)/Ag(100) film structures of excellent epitaxial quality.

It should be noted that our model is quite simple. Some systematic deviations between the experimental and the calculated hf field distributions, especially concerning the relative intensity of the ^{57}Fe probe atoms in the second layer ($n_1 = 0$, $n_2 = 1$ in Table 1), indicate that there may be present also steps of two- or even three-atomic height. On the other hand, recent band structure calculations of rough Fe/Cr *interfaces* demonstrated [24], that the magnetic moments of Fe and Cr show no significant dependence on their surrounding in contrast to the situation in *Fe-bulk material* containing Cr-impurities. So, our assumption that the Cr neighbors act virtually as magnetic holes in the n.n. or n.n.n. shell around the Fe ad-atom reducing the hf field by a nearly constant amount, seems to be reasonable. Nevertheless, independently of any models a simple look on the complex structure of the CEMS spectra shows, that the Fe/Cr interfaces of all our samples exhibit roughness which should be more pronounced as judged from LEED and RHEED. So, we suppose that our model gives a fairly realistic image of the interfaces despite the simplifications involved.

4. Conclusions

CEMS measurements on differently prepared epitaxial Fe(100)/Cr film structures in combination with a simple model for the evaluation of the spectra showed that there exists always a micro-roughness with island sizes of 1–2 nm due to chemical intermixing within 1–2 monolayers at the Fe/Cr interfaces. This micro-roughness could not be detected by RHEED and LEED analysis during the film preparation.

The aim of this study was to demonstrate the capability of CEMS for an analysis of interface roughness. A systematic or even quantitative comparison between roughness and type and strength of magnetic interlayer coupling was not possible due to the variety of the sample structures. So, with respect to magnetic coupling only a few general statements can be made. The chemical roughness does not seem to destroy the 180° interlayer coupling. Samples prepared at higher substrate temperatures (250°C) even revealed the short wave length ($\lambda \approx 2$ ML) oscillation of the coupling and in addition an increased contribution of 90° coupling. Because these samples showed a slightly increased interdiffusion, the mechanism of 90° coupling running via paramagnetic 'loose spins' in the nonmagnetic interlayer as suggested recently by Slonczewski is qualitatively supported.

References

[1] P. Grünberg, R. Schreiber, Y. Pang, M.B. Brodsky and H. Sowers, Phys. Rev. Lett. 57 (1986) 2442.
[2] M.N. Baibich, J.M. Broto, A. Fert, F. Nguyen van Dau, F. Petroff, P. Etienne, G. Creuzet and J. Chazelas, Phys. Rev. Lett. 61 (1988) 2471.
[3] G. Binasch, P. Grünberg, F. Saurenbach and W. Zinn, Phys. Rev. B 39 (1989) 4828.
[4] E.E. Fullerton, D.M. Kelly, J. Guimpel, I.K. Schuller and Y. Bruynseraede, Phys. Rev. Lett. 68 (1992) 859; T. Thomson, P.C. Riedi and D. Greig, Phys. Rev. B 50 (1994) 10319; Z.J. Yang and M.R. Scheinfein, Phys. Rev. B 52 (1995) 4263.
[5] J.C. Slonczewski, Phys. Rev. Lett. 67 (1991) 3172.
[6] S. Demokritov, E. Tsymbal, P. Grünberg, W. Zinn and I.K. Schuller, Phys. Rev. B 49 (1994) 720.
[7] J.C. Slonczewski, J. Appl. Phys. 73 (1993) 5957.
[8] C.F. Majkrzak, J.F. Ankner, N.F. Berk and D. Gibbs, in Magnetic Multilayers, eds. L.H. Bennett and R.E. Watson (World Scientific, Singapore, 1994) p. 299.
[9] A. Schreyer, J.F. Ankner, M. Schäfer, Th. Zeidler, H. Zabel, C.F. Majkrzak and P. Grünberg, J. Magn. Magn. Mater. 148 (1994) 189; Phys. Rev. B 52 (1995) 16066.
[10] N. Hosoito, K. Mibu, S. Araki, T. Shinjo, S. Itoh and Y. Endoh, J. Phys. Soc. Jpn. 61 (1992) 300.
[11] A. Kamijo and H. Igarashi, J. Appl. Phys. 71 (1992) 2455.
[12] P. Etienne, J. Massies, S. Lequien, R. Cabanel and F. Petroff, J. Cryst. Growth 111 (1991) 1003.
[13] R. Schad, C.D. Potter, P. Belien, G. Verbanck, V.V. Moshchalkov and Y. Bruynseraede, Appl. Phys. Lett. 64 (1994) 3500.
[14] J.A. Wolf, Q. Leng, R. Schreiber, P.A. Grünberg and W. Zinn, J. Magn. Magn. Mater. 121 (1993) 253.
[15] G. Gewinner, J.C. Peruchetti, A. Jaegle and R. Riedinger, Phys. Rev. Lett. 43 (1979) 935.
[16] J. Landes, Ch. Sauer, R.A. Brand, W. Zinn, S. Mantl and Zs. Kajcsos, J. Magn. Magn. Mater. 86 (1990) 71.
[17] A.M. Afanas'ev and E. Yu. Tsymbal, Hyperf. Interact. 62 (1990) 325.
[18] S.M. Dubiel and J. Zukrowski, J. Magn. Magn. Mater. 23 (1981) 214.
[19] J. Landes, Ch. Sauer, R.A. Brand, W. Zinn and Zs. Kajcsos, Hyperf. Interact. 57 (1990) 1941.
[20] J. Landes, Ch. Sauer, S. Dörrer and W. Zinn, J. Magn. Magn. Mater. 113 (1992) 137.
[21] J.A. Stroscio, D.T. Pierce and R.A. Dragoset, Phys. Rev. Lett. 70 (1993) 3615.
[22] D.T. Pierce, J.A. Stroscio, J. Unguris and R.J. Celotta, Phys. Rev. B 49 (1994) 14564.
[23] P.J. Schurer, Z. Celinski and B. Heinrich, J. Appl. Phys. 75 (1994) 5583; Phys. Rev. B 48 (1993) 2577; Phys. Rev. B 51 (1995) 2506.
[24] R. Coehoorn, J. Magn. Magn. Mater. 151 (1995) 341.